Day-to-day variations of migrating semidiurnal tide in the mesosphere and thermosphere

Yasunobu Miyoshi[1]* and Hitoshi Fujiwara[2]

[1]*Department of Earth and Planetary Sciences, Faculty of Sciences,*
Kyushu University, Fukuoka 812-8581
[2]*Department of Geophysics, Faculty of Science, Tohoku University, Sendai 980-8578*
Corresponding author. E-mail: miyoshi@geo.kyushu-u.ac.jp

Abstract: By using a general circulation model, we examine behavior of the migrating semidiurnal tide for solar cycle moderate and geomagnetically quiet conditions. We investigate day-to-day variabilities of the migrating semidiurnal tide in the mesosphere and thermosphere and their relation with the migrating semidiurnal tide generated in the lower atmosphere. The results show that day-to-day variations of the migrating semidiurnal tide are evident from the tropopause to the thermosphere. Fluctuations of the migrating semidiurnal amplitude with periods of 10–12 and 25 days are found at altitudes from 20 to 250 km, indicating dynamical coupling between the mesosphere and thermosphere and the lower atmosphere.

key words: semidiurnal tide, dynamical coupling, general circulation model

1. Introduction

The semidiurnal tide is one of the dominant components of the atmospheric motion in the mesosphere and lower thermosphere region (MLT). Observational and numerical studies have revealed that the amplitude of the semidiurnal tide has variability with a range from a few days to a decate (*e.g.*, solar cycle variability). For example, at middle and high latitudes, the semidiurnal amplitude in the MLT has seasonal variation, and a distinct peak of the amplitude appears in September. The semidiurnal amplitude at middle and high latitudes in the MLT is larger in winter than in summer. Furthermore, vertical wavelength of the semidiurnal tide is smaller in winter than in summer, indicating that higher mode such as (2,5) mode or (2,6) mode is dominant in winter. (*e.g.*, Manson *et al.*, 1989; Tsuda *et al.*, 1988). Variations of the semidiurnal amplitude with intraseasonal time scale (10–60 days) are also observed by many radars (*e.g.* Pancheva *et al.*, 2003). In this study, we focus our attention on day-to-day variations of the semidiurnal tide in the MLT.

Several mechanisms are considered to account for the variability of the semidiurnal tide in the MLT. Plausible sources of the variability of the semidiurnal tide are summarized as: (1) variations of forcing in the troposphere and stratosphere, (2) effects

of non-migrating tide, (3) effects of nonlinear interaction between the semidiurnal tide and other waves (such as planetary wave and gravity wave), (4) effects of changes in background wind and temperature in the stratosphere and mesosphere, and (5) changes in solar flux and/or geomagnetic activity.

Miyahara and Miyoshi (1997) showed that the amplitude of the non-migrating semidiurnal tide is non-negligible in the MLT (mechanism 2). Pancheva *et al*. (2002) investigated the nonlinear interaction between the 16-day wave and the migrating semidiurnal tide (mechanism 3). Pancheva *et al*. (2003) indicated a positive correlation between the solar activity and the variability of the semidiurnal amplitude and the total ozone (mechanism 5). Lindzen and Hong (1974), Aso *et al*. (1981) and Riggin *et al*. (2003) showed that changes in the background wind and temperature in the mesosphere influenced the semidiurnal amplitude (mechanism 4).

With regard to mechanism 1, Hagan (1996) showed that latent heat release associated with cloudiness or rainfall in the troposphere was a plausible source of the variability of the migrating semidiurnal tide in MLT. However, in Hagan's model, an annual mean distribution of latent heat release is used to investigate forcing of the semidiurnal tide. Effects of day-to-day variations of the general circulation in the troposphere on the semidiurnal tide amplitude in the upper atmosphere are not well known. Furthermore, observations of day-to-day variations of the semidiurnal tide are restricted in the MLT region, and day-to-day variations of the semidiurnal tide in the lower atmosphere (troposphere and stratosphere) and the upper thermosphere are not well known. Thus, mechanisms for day-to-day variations of the semidiurnal tide in the MLT are not clear.

In this study, we investigate day-to-day variations of the migrating semidiurnal tide in the mesosphere and thermosphere and their relation with the migrating semidiurnal tide generated in the lower atmosphere, by using a GCM which contains whole atmospheric regions; viz., the troposphere, stratosphere, mesosphere and thermosphere. The descriptions of the GCM used in this study and numerical simulation are presented in Section 2. Results and discussion are presented in Section 3. Summary follows in Section 4.

2.   Descriptions of the GCM and numerical simulation

The GCM used in this study is a global spectral model (T21) with 75 vertical levels, and contains the region from the ground surface to the exobase (about 500 km height). The GCM solves the full nonlinear primitive equations for eastward momentum, northward momentum, thermodynamics, continuity and hydrostatics. The detailed descriptions of the GCM are found in Miyoshi and Fujiwara (2003), so that the description of the GCM is briefly mentioned here.

In the troposphere, stratosphere and mesosphere, the GCM has a full set of the physical processes, such as radiation, a boundary layer, hydrology, moist and dry convection and eddy diffusion. Effects of the topography of the surface are also taken into account. The distributions of water vapor and cloud are predicted in the GCM. The monthly mean distribution of O_3 is adopted. Below 95 km height, effects of unsolved orographic and non-orographic gravity wave drags are parameterized by McFarlane (1987) and Lindzen (1981), respectively.

In the thermosphere, the GCM includes schemes for the infrared radiation, absorption of solar extreme ultraviolet and ultraviolet radiations, the ion drag force, the Joule heating, the auroral particle precipitation and the molecular diffusions of momentum and heat. The neutral composition in the thermosphere is obtained from the empirical model of MSIE90 (Hedin, 1991), and specified as a function of latitude and pressure. The global electron density distribution produced mainly by solar radiation is represented by the Chiu's empirical model (Chiu, 1975). In addition to electrons obtained by the Chiu's model, electrons produced by auroral particles are taken into account as described by Fuller-Rowell and Evans (1987) and Roble and Ridley (1987).

The time integration is conducted for solar cycle moderate (F10.7 cm solar flux = 135) and geomagnetically quiet (Ap = 4) conditions. The integrated data are sampled hourly for one year after the equilibrium state is realized. By using a space-time Fourier analysis (*e.g.*, Hayashi, 1971), amplitudes of the westward propagating semidiurnal component with zonal wavenumber 2, *i.e.*, the migrating semidiurnal tide are extracted. Because solar flux, the geomagnetic activity and ionospheric parameters are fixed during the numerical simulation, effects of day-to-day variations of solar flux and the geomagnetic activity on the migrating semidiurnal tide are excluded.

3.   Results and discussion

Figures 1a–1b show the latitude-height cross section of the monthly mean amplitude of the migrating semidiurnal tide in March. The amplitude of the zonal and meridional components is 10–15 m/s at 80 km height, and the amplitude between 90–120 km increases rapidly with height. The maximum amplitude at middle latitudes and at low latitudes is located at 120 and at 140 km height, respectively. The maximum value in the lower thermosphere is about 60 m/s. The latitudinal structure of the semidiurnal amplitude is symmetric with respect to the equator.

Figures 2a–2b show the monthly mean amplitude of the migrating semidiurnal tide in January. The large amplitude is found at high latitudes of the winter hemisphere. The amplitude between 80–140 km is larger in winter than in summer. At low latitudes above 120 km height, the amplitude in January is quite similar to that in March. Figure 3 shows the time-height cross section of deviation of the zonal wind from diurnal mean zonal wind at $0°$E and $58°$N in January. This latitude is chosen since the migrating semidiurnal amplitude in the MLT has a maximum around $60°$ latitude. As might be expected, the zonal wind has a pronounced semidiurnal variation between 80 and 140 km heights, while the in-situ diurnal tide becomes dominant above 150 km height. Below 110 km height, amplitude of a semidiurnal wind variation increases with increasing height, and approaches 80 m/s at 110 km. The phase lines descend with time, and show a vertical wavelength of about 40–45 km. These are characteristic of the upward propagating migrating semidiurnal tide. These features of the semidiurnal tide obtained by the GCM are consistent with the observations (*e.g.*, Manson *et al.*, 1989). Hence, the GCM is quite useful for studying the semidiurnal tide.

We investigate temporal variability of the migrating semidiurnal tide amplitude at various heights. Figures 4a–4f show time series of the amplitude of the migrating semidiurnal zonal wind component at $58°$N at the altitudes of (a) 20 km, (b) 50 km, (c)
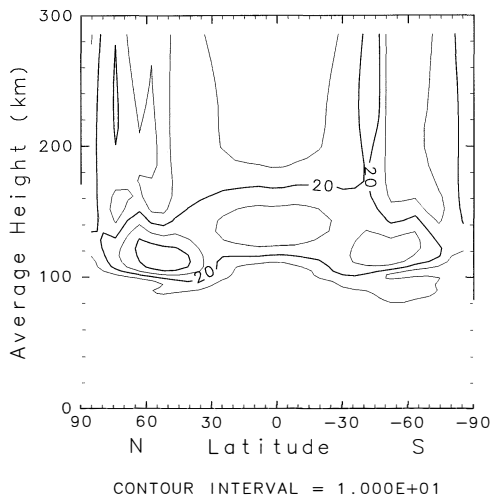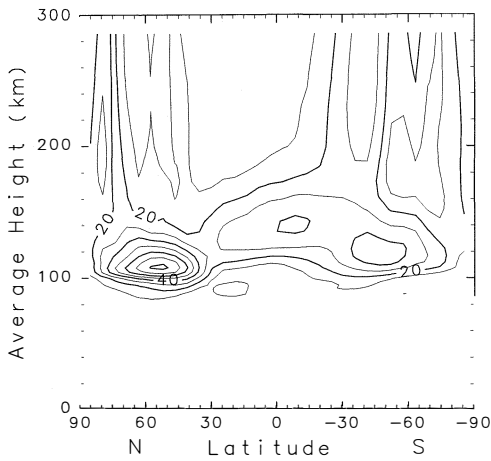
CONTOUR INTERVAL = 1.000E+01

Fig. 1a. *Latitude-height plot of the monthly mean amplitude of the migrating semidiurnal zonal wind component in March. Contour interval is 10 m/s.*
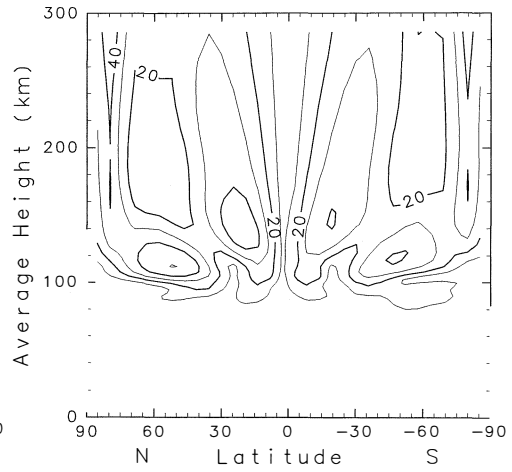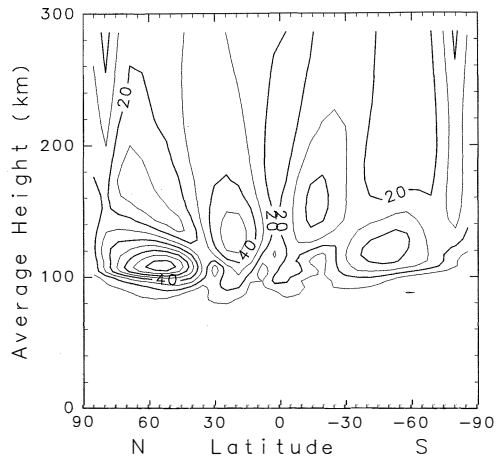
Fig. 1b. *As in Fig. 1a but for the meridional wind component.*

CONTOUR INTERVAL = 1.000E+01

Fig. 2a. *Latitude-height plot of the monthly mean amplitude of the migrating semidiurnal zonal wind component in January. Contour interval is 10 m/s.*

Fig. 2b. *As in Fig. 2a but for the meridional wind component.*

CONTOUR INTERVAL = 2.000E+01

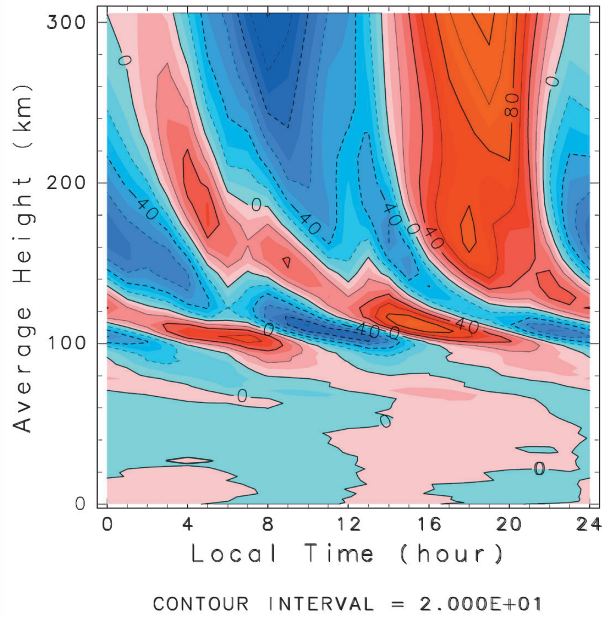*Fig. 3. Local time-height plot of deviation of the zonal wind from diurnal mean zonal wind at 0°E longitude and 58°N latitude. Contour interval is 20 m/s. Positive and negative values indicate eastward and westward winds, respectively.*
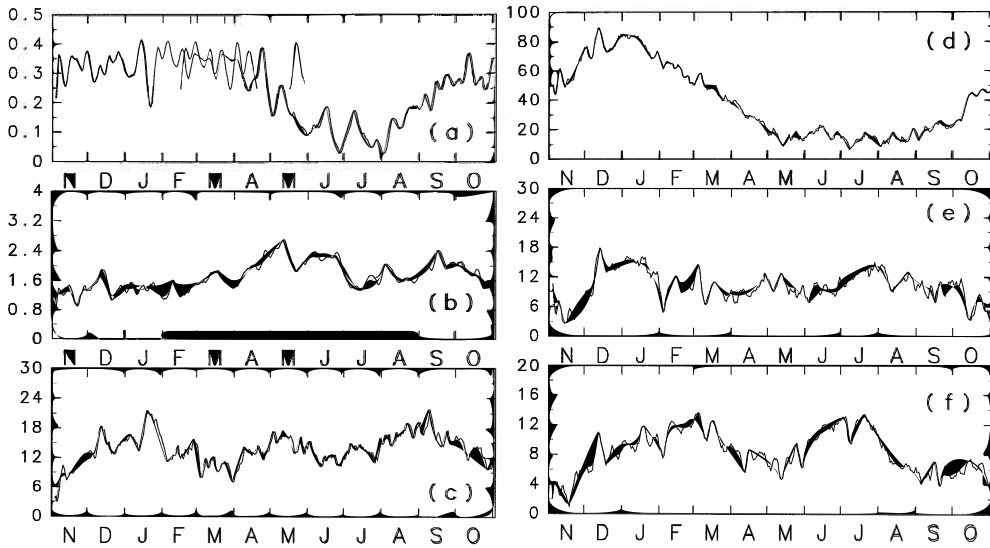

Fig. 4. Time series of amplitudes of the migrating semidiurnal zonal wind component at 58°N in January. Each panel shows the time series at the altitudes of (a) 20 km, (b) 50 km, (c) 90 km, (d) 110 km, (e) 170 km and (f) 250 km with unit of m/s.

90 km, (d) 110 km, (e) 170 km, (f) 250 km, respectively.   The amplitude of the migrating semidiurnal tide is small at 20 and 50 km hights, however, day-to-day variations of the amplitude are clearly seen.   The amplitude at 90 and 110 km heights indicates marked day-to-day variations.   For example, the amplitude at 110 km height in winter ranges from 50 to 90 m/s, while the amplitude at 90 km height in winter ranges from 10 to 24 m/s.   The migrating semidiurnal tide amplitude in the upper thermosphere also shows day-to-day variation.   Although solar flux, the geomagnetic activity and ionospheric parameters are fixed during the numerical simulation, day-to-day variations of the migrating semidiurnal tide amplitude are evident in the thermosphere, indicating dynamical coupling between the thermosphere and the lower atmosphere.   At middle and high latitudes, the amplitudes of the migrating semidiurnal meridional wind and temperature components also have similar day-to-day variations (not shown).

In order to investigate dominant periods of day-to-day variations of the migrating semidiurnal tide amplitude, a spectral analysis is performed.   Figures 5a–5c show power spectra of the migrating semidiurnal zonal wind component for 20, 50, and 90 km heights at 58°N.   Spectral peaks centered at 10–12 and 25 days are evident at all height ranges.   Other peaks centered at 15 and 31–32 days appear at 50 and 90 km heights. At 20 km height, spectral peaks at 16–17 and 20 days are also found.   It is noteworthy that the similar periodicities of 10–12 and 25 days are found in the height range from 20 to 90 km heights.   Spectral peaks at 10–12 and 25 days are also found in the upper thermosphere.

The migrating semidiurnal tide is generated in the troposphere and stratosphere, and propagates toward the MLT.   The fact that fluctuations of the migrating semidiurnal amplitude with periods of 10–12 and 25 days are found at altitudes from 20 to 250
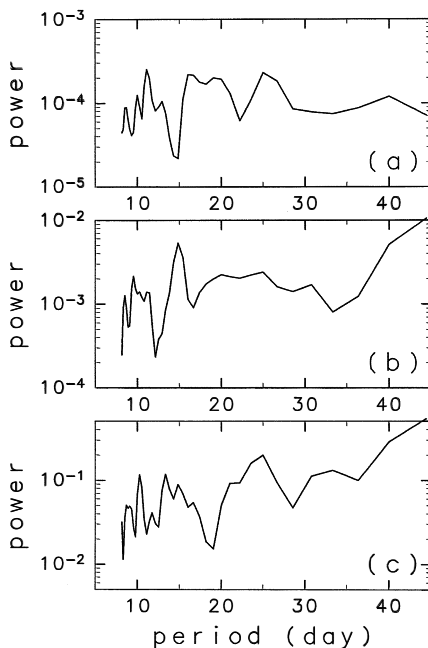

Fig. 5.   Power spectra of the migrating semidiurnal zonal wind amplitude at 58°N at altitudes of (a) 20 km, (b) 50 km, (c) 90 km.   Units are $m^2/s^2 \cdot day$.
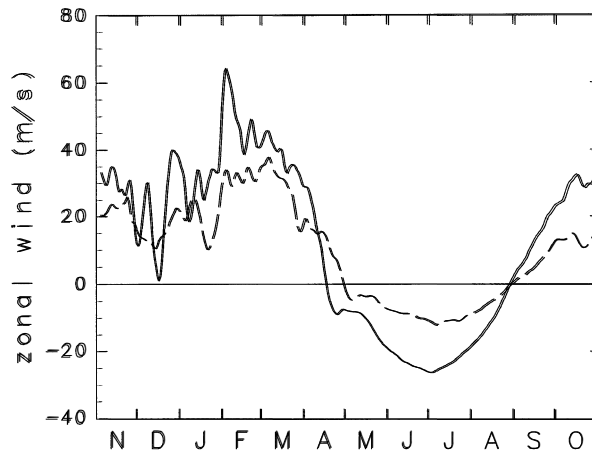
Fig. 6.   Time series of the zonal mean zonal wind at 58°N.   Solid and broken lines show the zonal wind at 50 km height and 30 km height, respectively.   Units are m/s.

km indicates that the semidiurnal amplitude in the mesosphere and thermosphere is influenced by the semidiurnal migrating tide generated in the lower atmosphere.   Next, effects of variations of the general circulation in the stratosphere on the tidal variability in the MLT are examined.   Figure 6 shows time series of the zonal mean zonal wind at 58°N in the stratosphere.   In winter and spring, day-to-day variations of planetary wave activity of the stratosphere are very large and affect the zonal mean wind.   The zonal mean zonal wind in the stratosphere fluctuates with periods of 10–30 days.   In the summer stratosphere, upward propagation of the stationary planetary wave from the troposphere is prohibited due to the easterly wind, and planetary wave activity is negligibly small.   Day-to-day variations of the zonal mean zonal wind also disappear in the summer stratosphere.   However, day-today variations of the migrating semidiurnal tide amplitude in the stratosphere and MLT are clearly seen not only in winter but also in summer.   These results indicate that day-to-day variations of the semidiurnal migrating tide amplitude in summer are generated in the troposphere.

   Day-to-day variations of the migrating semidiurnal tide amplitude are evident from the lower stratosphere to the upper thermosphere.   The distributions of water vapor and cloud in the troposphere have day-to-day variations, and these variations influence forcing of the semidiurnal tide due to the absorption of the solar radiation in the troposphere.   In addition, Hagan (1996) suggested that latent heat release associated with cloudiness and rainfall was another source for the migrating semidiurnal tide. Thus, variability of water vapor and cloud affects excitation of the migrating semidiurnal tide in the troposphere.   These results suggest that day-to-day variations of the general circulation in the troposphere influence the migrating semidiurnal amplitude in the mesosphere and thermosphere.

4. Summary

By using the GCM which contains the region from the ground surface to the exobase, day-to-day variations of the migrating semidiurnal tide amplitude are investigated. Although solar flux, the geomagnetic activity and ionospheric parameters are fixed during the numerical simulation, day-to-day variations of the migrating semidiurnal tide amplitude are evident from the tropopause to the upper thermosphere. The fact that fluctuations of the migrating semidiurnal amplitude with periods of 10–12 and 25 days are found at altitudes from 20 to 250 km suggests that the migrating semidiurnal amplitude in the mesosphere and thermosphere is influenced by the semidiurnal migrating tide generated in the lower atmosphere.

In this study, we investigated the semidiurnal tide under the conditions of the constant solar EUV and UV fluxes and the geomagnetic activity. We will evaluate the variability of the semidiurnal tide in the presence of day-to-day variations of the EUV, UV fluxes, geomagnetic activity and ionospheric parameters in the next step.

Acknowledgments

References

Aso, T., Nonoyama, T. and Kato, S. (1981): Numerical simulation of semidiurnal atmospheric tides. J. Geophys. Res., **86**, 11388–11400.

Chiu, Y.T. (1975): An improved phenomenological model of ionospheric density. J. Atmos. Terr. Phys., **37**, 1563–1570.

Forbes, J.M. (1982): Atmospheric Tides 2. The solar and lunar semidiurnal components. J. Geophys. Res., **87**, 5241–5252.

Fuller-Rowell, T.J. and Evans, D.S. (1987): Height-integrated Pedersen and Hall conductivity patterns inferred from the TIROS-NOAA satellite data. J. Geophys. Res., **92**, 7606–7618.

Hagan, M.E. (1996): Comparative effects of migrating solar sources on tidal signatures in the middle and upper atmosphere. J. Goephys. Res., **101**, 21213–21222.

Hayashi, Y. (1971); A generalized method of resolving disturbances into progressive and retrogressive waves by space Fourier and time cross-spectral analyses. J. Meteorol. Soc. Jpn., **49**, 125–128.

Hedin, A.E. (1991): Extension of the thermosphere model into the middle and lower atmosphere. J. Geophys. Res., **96**, 1159–1172.

Lindzen, R.S. (1981): Turbulence and stress owing to gravity wave and tidal breakdown. J. Geophys. Res., **86**, 9707–9714.

Lindzen, R.S. and Hong, S. (1974): Effects of mean winds and horizontal temperature gradients on solar and lunar semidiurnal tides in the atmosphere. J. Atmos. Sci., **31**, 1421–1446.

McFarlane, N.A. (1987): The effect of orographically excited gravity wave drag on the general circulation of the lower stratosphere and troposphere. J. Atmos. Sci., **44**, 1775–1800.

Manson, A.H., Meek, C.E., Teitelbaum, H., Vial, F., Schminder, R., KürSchner, D., Smith, M.J., Fraser, G. J. and Clark, R.R. (1989): Climatologies of semi-diurnal and diurnal tides in the middle atmosphere (70–110 km) at middle latitudes (40–55°). J. Atmos. Terr. Phys., **51**, 579–593.

Miyahara, S. and Miyoshi, Y. (1997): Migrating and non-migrating atmospheric tides simulated by a middle atmosphere general circulation model. Adv. Space Res., **20**, 1201–1207.

Miyoshi, Y. and Fujiwara, H. (2003): Day-to-day variations of migrating diurnal tide simulated by a GCM from the ground surface to the exobase. Geophys. Res. Lett., **30**, 1789, doi: 10.1029/2003GL017695.

Pancheva, D., Mitchell, N., Clark, R.R., Drobjeva, J. and Lastovicka, J. (2002): Variability in the maximum height of the ionospheric F2-layer over Millstone Hill (September 1998–March 2000); influence from below and above. Ann. Geophys., **20**, 1807–1819.

Pancheva, D., Mitchell, N., Middleton, H. and Muller, H. (2003): Variability of the semidiurnal tide due to fluctuations in solar activity and total ozone. J. Atmos. Solar-Terr. Phys., **65**, 1–19.

Riggin, D.M., Meyer, C.K., Fritts, D.C., Jarvis, M.J., Murayama, Y., Singer, W., Vincent, R.A. and Murphy, D.J. (2003): MF radar observations of seasonal variability of semidiurnal motions in the mesosphere at high northern and southern latitudes. J. Atmos. Solar-Terr. Phys., **65**, 483–393.

Roble, R.G. and Ridley, E.C. (1987): An auroral model for the NCAR thermospheric general circulation model (TGCM). Ann. Geophys., **54**, 369–382.

Tsuda, T., Kato, S., Manson, A.H. and Meek, C.E. (1998): Characteristics of semidiurnal tides observed by the Kyoto Meteor Radar and Saskatoon Medium-Frequency Radar. J. Geophys. Res., **93**, 7027–7036.